

Remote Control on the Photochemical Rearrangement of 1,6-(*N*-Aryl)aza-[60]fulleroids to 1,2-(*N*-Arylaziridino)-[60]fullerenes by *N*-Substituted Aryl Groups

Akihiko Ouchi,^{*,†} Bahlul Z. S. Awen,[†] Ryota Hatsuda,[†] Reiko Ogura,[‡] Tadahiro Ishii,[‡] Yasuyuki Araki,[§] and Osamu Ito^{*,§}

National Institute of Advanced Industrial Science and Technology (AIST), Tsukuba, Ibaraki 305-8565, Japan; Faculty of Science, Tokyo University of Science, Kagurazaka, Tokyo 162-8601, Japan; and the Institute of Multidisciplinary Research for Advanced Materials, Tohoku University, Sendai, Miyagi 980-8577, Japan

Received: June 23, 2004; In Final Form: August 25, 2004

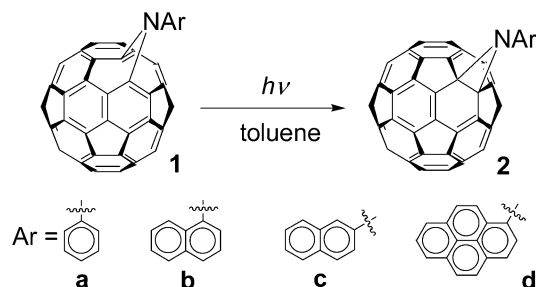
Photochemical rearrangement of 1,6-(*N*-aryl)aza-[60]fulleroids (**1**) to 1,2-(*N*-arylaziridino)-[60]fullerenes (**2**) depends on the *N*-aryl substituents remote from the reaction center. A systematic kinetic study of the *N*-substituents discloses a decrease in the reaction rates of the photochemical rearrangement in the order 1-naphthyl (**1b**) > 1-pyrenyl (**1d**) > phenyl (**1a**) > 2-naphthyl (**1c**). The large substituent effect in the rates, which vary by ca. 2200-fold, is interpreted in terms of changes in the reaction mechanisms. The fast photochemical rearrangement of derivatives **1b,d** proceeds through the normal triplet states of **1**; in the case of **1b**, triplet sensitization by the product **2b** also operates. For the slow rearrangement rates of **1a,c**, nanosecond transient absorption spectroscopy reveals that different triplet states participate, namely, electron transfer between the *N*-aryl substituent and the fullerene.

Introduction

In recent years, chemical modification of C₆₀ became increasingly important as a tool for the functionalization of fullerenes to add new functions to the parent fullerene molecules. Many thermal and photochemical reactions have been developed for the efficient chemical modification of fullerenes.^{1,2} One of the widely used reactions is that of fullerenes with organic azides,^{3,4} which has been extensively employed for the preparation of functional fullerene derivatives⁵ and for the incorporation of fullerenes into various polymers.⁶ Both thermal and photochemical processes have been reported for this reaction. For C₆₀ molecules, the thermal reaction proceeds by initial 1,3-dipolar cycloaddition of the azide to the double bonds of C₆₀, followed by nitrogen elimination to form 1,6-(*N*-substituted)-aza-[60]fulleroids (**1**),³ whereas the photochemical reaction proceeds by the initial generation of nitrenes and their addition to the double bonds of C₆₀ to form 1,2-(*N*-substituted-aziridino)-[60]fullerenes (**2**).³

The photochemical conversion **1** → **2** (Scheme 1) is also often used in the chemical modification of C₆₀,^{3–6} but the details on the scope and limitations of this reaction are not known. A spectroscopic study of **1** and **2** with alkyl substituent, e.g., the methoxyethoxymethyl (MEM) group, has been conducted, and an interaction between the electron pair of the nitrogen atom and the fullerene π-electron system was found.⁷ If the interaction between the nitrogen atom and the C₆₀ moiety of **1** and **2** is due to the nitrogen electron pair, a similar reactivity would be expected for the photochemical rearrangement **1** → **2**, regardless of the type of *N*-substituents used. Nonetheless, a striking effect of the *N*-substituent has been reported in the photochemical rearrangement, e.g., whereas 1,6-(*N*-methoxyethoxymethyl)aza-

SCHEME 1



[60]fulleroid (**1**, Ar = MEM) is photochemically inactive,^{3c} 1,6-(*N*-phenyl)aza-[60]fulleroid (**1a**) rearranges photochemically into **2a**.^{3g} This result indicates additional features that play an important role in the photochemical reactivity of **1**. Although photochemical rearrangements of the carbon analogues, i.e., fulleroids to methanofullerenes,⁸ have been carried out, systematic studies on the substituent effects of the bridged carbon atom have not been reported so far. This remote control of the reaction is most likely due to interactions between the *N*-aryl substituents that are not directly connected to the reaction center and the C₆₀ moiety.

For this reaction to be useful in the preparation of novel materials, it is necessary to understand the nature of this remote controlling effect of the *N*-substituted aryl groups. If the photochemical properties of the fullerene derivatives may be manipulated by appropriate *N*-substituents, such fullerene derivatives may find valuable applications in material science.

Therefore, we have conducted a systematic study on the photochemical rearrangement **1** → **2** with different *N*-aryl substituents (Scheme 1),⁹ namely, the phenyl (**a**),^{3g} 1-naphthyl (**b**), 2-naphthyl (**c**), and 1-pyrenyl (**d**) groups. Indeed, the difference in the photochemical rearrangement rates was found to be more than 2000-fold between the fastest (**1b**) and slowest (**1c**). This rate effect is attributed to switching between two

[†] National Institute of Advanced Industrial Science and Technology (AIST).

[‡] Tokyo University of Science.

[§] Tohoku University.

* Corresponding author. E-mail: ouchi.akihiko@aist.go.jp.

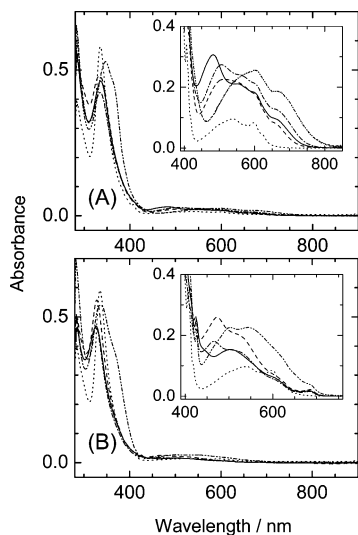


Figure 1. (A) Absorption spectra of **1a–d** and C_{60} and (B) **2a–d** and C_{60} . Concentration: 10^{-5} and 10^{-4} M (insets) in toluene. Codification of substrates and products: **1a, 2a** (—); **1b, 2b** (---); **1c, 2c** (- · - ·); **1d, 2d** (- · · -); C_{60} (···).

different excited states due to the structural difference of the *N*-substituents. Such a phenomenon may be applied to molecules other than fullerene derivatives and has potential for exploring new chemistry. We presently report on the details of our triplet sensitization, spectroscopic, and kinetic experiments.

Results

Steady-State Absorption and Fluorescence Spectra of 1 and 2. Compounds **1** and **2** were synthesized from C_{60} and the corresponding aryl azides as reported previously.⁹ Parts A and B of Figure 1 show absorption spectra of **1a–d** and **2a–d**, respectively, together with that of C_{60} . Both figures show strong absorptions at <430 nm and weak absorptions at >430 nm. In analogy to C_{60} ,¹¹ the absorptions of **1a–d** and **2a–d** at <430 nm can be assigned to the allowed and the weak absorptions at >430 nm to the forbidden transitions.

On comparison of these spectra with that of the parent C_{60} , a considerable increase in the absorption intensity of the forbidden transition bands was observed for both **1** and **2**. The increase of the absorption intensities of **2a–d** at >400 nm was 1.8–2.7-fold compared with that of the parent C_{60} . This increase is due to the interactions caused by direct bonding of C_{60} and arylamine groups because mixtures of *N,N*-dimethyl- or *N,N*-diethylanilines and C_{60} in decalin do not show any considerable change in their absorption intensities.¹² One of the effects of the direct bonding is the decrease of the symmetry of C_{60} . The pattern of the absorption bands, for both **1** and **2**, is also slightly influenced by the difference of the substituents.

The absorption spectra of **1** at >430 nm also showed a considerable red shift compared with those of **2**, particularly in the case of **1d**, which can be rationalized by the increase of the number of π -electrons from 60 to 62 electrons.⁷ The small sharp absorption that corresponds to the λ_{\max} at 407 nm of C_{60} was not observed in **1a–d**, but the corresponding absorption appeared at ca. 424 nm for **2**.

Parts A and B of Figure 2 show fluorescence spectra of **1a–d** and **2a–d**, respectively. Although the intensity of the fluorescence spectra was different, the shapes of the spectra of **1b,d** and **2a–d** were very similar to each other. The spectra showed an emission maximum at 695 nm and shoulders at 760 and 800 nm, which is very similar to those of 1,2-substituted C_{60}

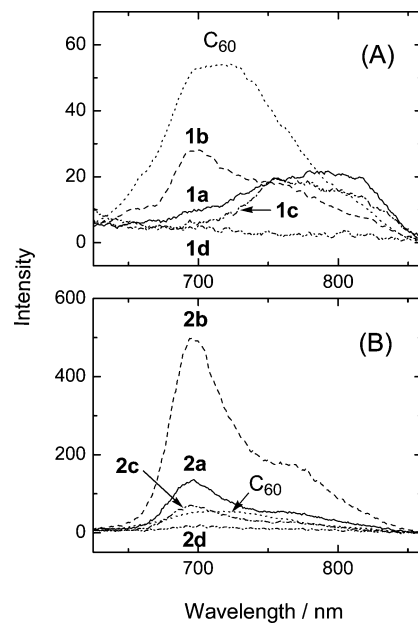


Figure 2. (A) Fluorescence spectra of **1a–d** and C_{60} and (B) **2a–d** and C_{60} in toluene at room temperature. Concentration: 10^{-4} M (**1a–c**, **2a–d**, and C_{60}) and saturated solution (**1d**, between 5×10^{-5} and 10^{-4} M). Excitation wavelength: 500 nm with bandpath 15 nm and emission bandpath 20 nm. All emission spectra were recorded by setting 580 nm cut filter in the emission pathway. Codification of substrates and products: **1a, 2a** (—); **1b, 2b** (---); **1c, 2c** (- · - ·); **1d, 2d** (- · · -); C_{60} (···).

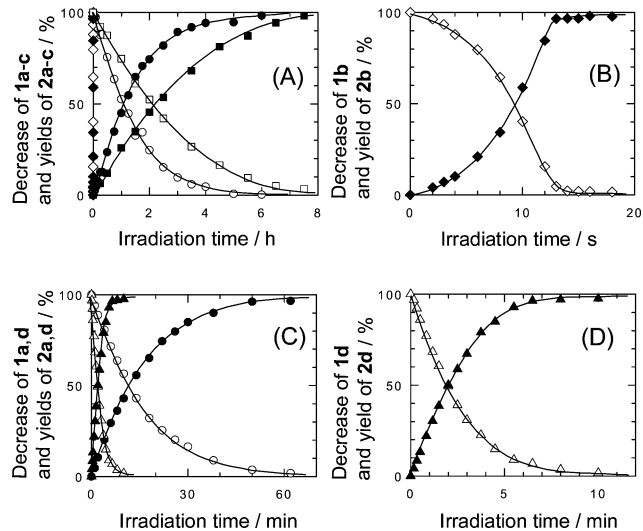


Figure 3. (A) Decrease of **1a–c** and formation of **2a–c**,^{14c} (B) of **1b** and **2b**,^{14d} (C) of **1a,d** and **2a,d**,^{14c} and (D) of **1d** and **2d**^{14c} in degassed solutions as a function of irradiation time. Codification of substrates **1a** (○), **1b** (◇), **1c** (□), **1d** (△) and products **2a** (●), **2b** (◆), **2c** (■), **2d** (▲). Concentration: (A, B) 5×10^{-4} M and (C, D) 1×10^{-5} M **1** in toluene; light source: 500 W Xe lamp, fitted with a water filter and a Toshiba UV-29 filter (>290 nm light).

derivatives, such as pyrrolidinofullerenes.¹³ In contrast, the fluorescence spectra of **1a** and **1c** were quite different from the others; the spectra had emission maxima at 760 and 800 nm and a shoulder at 695 nm. This red shift of the fluorescence emission was also observed in the *N*-MEM-substituted **1**.⁷

Photochemical Rearrangement 1 → 2. Figure 3 shows the time profiles of photochemical rearrangement **1** → **2** by irradiation with >290 nm light under nitrogen atmosphere, which were determined by HPLC analyses. The figure shows the decrease of **1a–d** and the increase of **2a–d** as a function of irradiation time. The reaction proceeded quantitatively for

all substituents without the formation of byproducts. The light is mainly absorbed by the allowed transitions of **1a–d** at 290–400 nm, and as seen in Figure 1a, the molar absorption coefficients (ϵ) of **1a–d** were similar to each other in this wavelength region: ϵ of **1a–d** at 290 nm and λ_{max} were 46 800 and 46 100 $\text{M}^{-1} \text{cm}^{-1}$ (336 nm) for **1a**, 49 200 and 48 000 (334 nm) $\text{M}^{-1} \text{cm}^{-1}$ for **1b**, 50 500 and 42 300 (334 nm) $\text{M}^{-1} \text{cm}^{-1}$ for **1c**, and 51 200 and 52 900 (347 nm) $\text{M}^{-1} \text{cm}^{-1}$ for **1d**.

As seen in Figure 3A, the consumption of **1a,c** and the formation of **2a,c** showed exponential-like decay and rise, which is an indication for a unimolecular process. The reaction was completed after 6 h for **1a** and 8 h for **1c**, whereas for **1b** the reaction was complete in only 13 s. In addition, an induction period was observed in the reaction of **1b**, which exhibited nonexponential-like curves for the consumption of **1b** and the formation of **2b** (cf. Figure 3B). Control experiments showed no decomposition of **2a–d** under the same photolysis conditions as those of **1a–d**, which indicates that the yield of **2a–d** was not affected by the secondary reactions of **2a–d** or by the reverse reactions **2** \rightarrow **1**. The photolysis of **1d** had to be conducted at lower concentrations because of its low solubility; thus, for comparison (cf. Figure 3C), the photolysis of **1a** was also run at low concentration. As seen in Figure 3C, the reaction was completed after 60 min for **1a** and 10 min for **1d**. Figure 3D also displays the exponential-like decay and rise in the photolysis of **1d**, which is an indication for a unimolecular process. The required reaction time for complete consumption of **1** followed the relative order **1a:1b:1c:1d** = 1660:1:2220:280.

The photolyses of **1a–d** in air-saturated solutions showed a large decrease in the rate of photochemical rearrangement **1** \rightarrow **2**.¹⁵ The photolyses were very sensitive to small amounts of oxygen; bubbling of nitrogen gas for 2 h through the reactant solution prior to the photolysis was not sufficient for the complete removal of oxygen, and the photolysis rate was considerably decreased.¹⁵ This indicates that the photolysis proceeded through triplet states of **1**, which is consistent with the report that the intersystem crossing (ISC) of C_{60} and its derivatives to their triplet states is very fast and efficient^{2b,16} and also that the oxygen quenching is diffusion-controlled.¹³

Wavelength Effect in the Photochemical Rearrangement 1 \rightarrow 2. The photolysis of **1** by >290 nm light proceeds mainly through the excitation to the allowed electronic transition states at 290–400 nm. The irradiations were also conducted by >600 nm light to investigate how the excitation through forbidden transitions affects the reaction. As seen in Figure 1A, >600 nm light is mainly absorbed in the longer wavelength region of the forbidden transition. The maximum molar absorption coefficients (ϵ) of **1a–d** at >600 nm are 1830 $\text{M}^{-1} \text{cm}^{-1}$ for **1a**, 1780 $\text{M}^{-1} \text{cm}^{-1}$ for **1b**, 2130 $\text{M}^{-1} \text{cm}^{-1}$ for **1c**, and 2590 $\text{M}^{-1} \text{cm}^{-1}$ for **1d**; thus, the absorption coefficients are similar at this wavelength.

Figure 4 shows the time profiles for the photochemical rearrangement **1** \rightarrow **2** by >600 nm light irradiation under a nitrogen atmosphere. The figure shows the decrease of **1a–d** and the increase of **2a–d** as a function of irradiation time; the features are similar to the reaction with >290 nm light, except for the slow reaction rate. The slow rate may be explained by the smaller ϵ values compared with those for >290 nm light. The exponential-like reaction was completed after 20 h for **1a** and 30 h for **1c** (Figure 4A), whereas a fast nonexponential-like reaction was observed for **1b**, which required only 50 s irradiation time for completion (Figure 4B). The photolyses of **1a** and **1d** were conducted at lower concentration, whose reaction time for completion was 6 h for **1a** and 1.3 h for **1d**

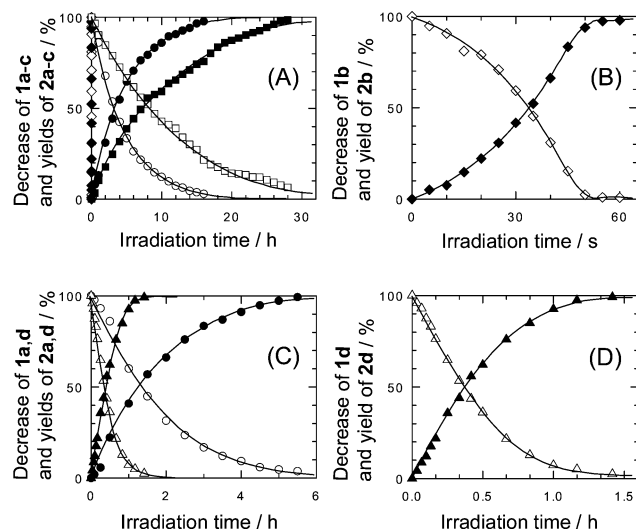


Figure 4. (A) Decrease of **1a–c** and formation of **2a–c**, (B) of **1b** and **2b**, (C) of **1a,d** and **2a,d**, and (D) of **1d** and **2d** in degassed solutions as a function of irradiation time.^{14a} Codification of substrates **1a** (○), **1b** (◇), **1c** (□), **1d** (△) and products **2a** (●), **2b** (◆), **2c** (■), **2d** (▲). Concentration: (A, B) 5×10^{-4} M and (C, D) 1×10^{-5} M **1** in toluene; light source: 500 W Xe lamp, fitted with a water filter and a Toshiba R-60 filter (>600 nm light).

(cf. parts C and D of Figure 4). The relative order of the required reaction time for complete rearrangement of **1** is **1a:1b:1c:1d** = 1440:1:2160:312, which is similar to the photolysis with >290 nm light. The photolysis of **1a–d** with >450 nm light also shows the same trend.¹⁵

Sensitization Effects in Photochemical Rearrangement 1 \rightarrow 2. Figures 3B and 4B show that the photochemical rearrangement **1b** \rightarrow **2b** is not a simple unimolecular reaction. The absence of secondary reactions of **2a–d** was confirmed under the same photolysis condition as those for **1a–d**. Therefore, we have interpreted the nonexponential-like feature of the reaction as triplet sensitization by the product **2b**. To confirm the sensitization effect of **2** and to estimate the relative triplet-state energy levels of **1** and **2**, we have conducted experiments on the effect of addition of authentic **2** in the photochemical rearrangement **1** \rightarrow **2**.

Figure 5 shows the consumption of **1** and the formation of **2** as a function of the ratio of the amount of initially added authentic **2** to **1**. In the case of **1b**, a large increase in the consumption of **1b** and the formation of **2b** is observed, which depends linearly on the amount of initially added authentic **2b**. Thus, the rate of the rearrangement increases with the progress of the reaction, which is consistent with the time profile of the rearrangement **1b** \rightarrow **2b** (cf. Figures 3B and 4B). The same effect was also observed when the photolysis was conducted with >600 nm light.¹⁵ On the contrary, in the cases of **1a,c,d**, the addition of authentic **2a,c,d** showed no effect on the consumption of **1a,c,d** and the formation of **2a,c,d**.

The relative triplet energy levels of **1** and **2** were determined by the photosensitized reactions using **2**; some of the results are exhibited in Figures 6–8. The addition of **2b–d** and C_{60} does not affect the photochemical rearrangement **1a** \rightarrow **2a**.¹⁵ In contrast, Figure 6 shows that the addition of C_{60} accelerates considerably the photochemical rearrangement **1b** \rightarrow **2b**, but **2a,c,d** do not.¹⁵ The consumption of **1b** and the formation of **2b** depended linearly on the amount of initially added C_{60} . Figure 7B also displays a considerable acceleration of the photochemical rearrangement **1c** \rightarrow **2c** when C_{60} was added, and the rate was slightly accelerated in the addition of **2b** (Figure

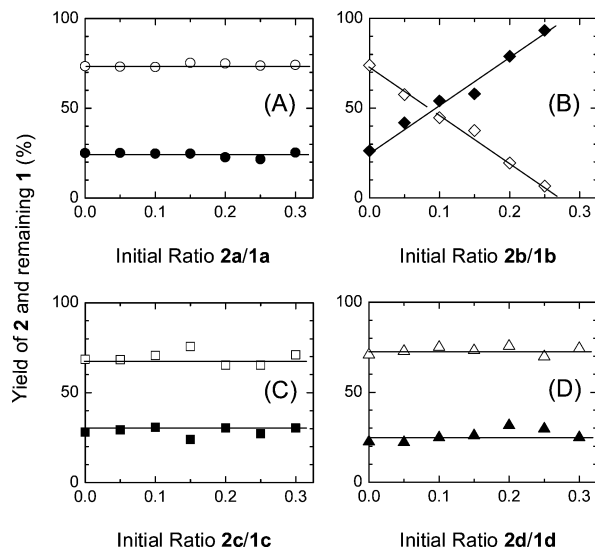


Figure 5. (A) Yield of **2a** and remaining **1a**, (B) of **2b** and **1b**, (C) of **2c** and **1c**, and (D) of **2d** and **1d** in degassed solutions as a function of the ratio of the amount of initially added authentic **2** to **1**.^{14a} Codification of substrates **1a** (○), **1b** (◇), **1c** (□), **1d** (△) and products **2a** (●), **2b** (◆), **2c** (■), **2d** (▲). Irradiation time: (A) 20 min, (B) 6 s, (C) 1 h, and (D) 50 s. Concentration: (A–C) 5×10^{-4} and (D) 1×10^{-5} M **1** in toluene. Light source: 500 W Xe lamp, fitted with a water filter and a Toshiba UV-29 filter (>290 nm light).

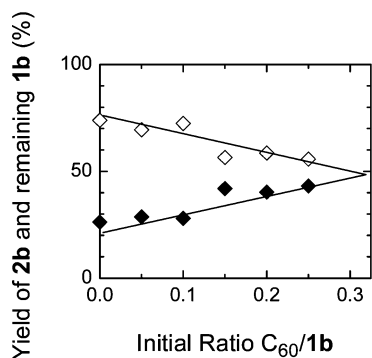


Figure 6. Yield of **2b** and remaining **1b** in degassed solutions as a function of the ratio of the amount of initially added authentic C_{60} to **1b**.^{14a} Codification of substrate **1b** (◇) and product **2b** (◆). Irradiation time: 6 s. Concentration: 5×10^{-4} M **1a** in toluene. Light source: 500 W Xe lamp, fitted with a water filter and a Toshiba UV-29 filter (>290 nm light).

7A); however, no rate effect was observed during the addition of **2a,d**.¹⁵ Figure 8 reveals in the photochemical rearrangement **1d** → **2d** a large acceleration for the addition of **2b** and C_{60} (the rearrangement terminates by 50 s irradiation when the initial ratio $C_{60}/1d$ is >0.15), a small one for **2c**, and no effect for **2a**.

Transient Spectra of Substrate 1 and Product 2. The difference of the reaction rates between **1a–d**, shown in Figures 3 and 4, cannot be explained by the molar extinction coefficients (ϵ) because the ϵ values are very similar in the >290 nm region and in the >600 nm region they vary only ca. 1.5-fold (Figure 1). Therefore, the large variation in the reactivity of **1a–d** suggested differences in the type of excited states involved. To scrutinize this possibility, we have measured nanosecond transient spectra of **1** and **2** in toluene (Figures 9 and 10).

Figure 9B-1 is the transient absorption spectrum of **1b**, which displays a *normal triplet* peak at 700 nm; the position and the shape of the peak were the same as those of reported fullerene derivatives.^{17,18} This fact suggests that the fast photochemical rearrangement **1b** → **2b** proceeds through normal triplet state(s). Derivative **1d** also rearranged fast, but it was difficult to measure

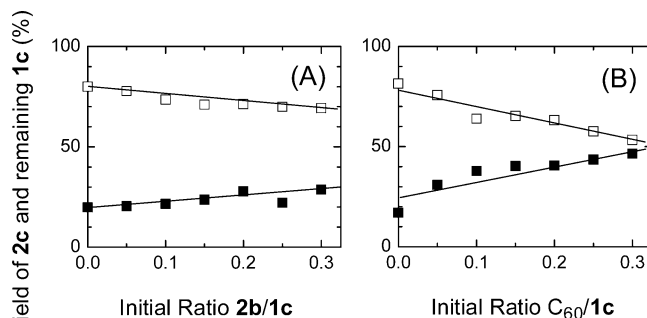


Figure 7. Yield of **2c** and remaining **1c** in degassed solutions as a function of the ratio of the amount of initially added authentic **2b** to **1c** (A)^{14a} and C_{60} to **1c** (B).^{14a} Codification of substrate **1c** (□) and product **2c** (■). Irradiation time: 1 h. Concentration: 5×10^{-4} M **1c** in toluene. Light source: 500 W Xe lamp, fitted with a water filter and a Toshiba UV-29 filter (>290 nm light).

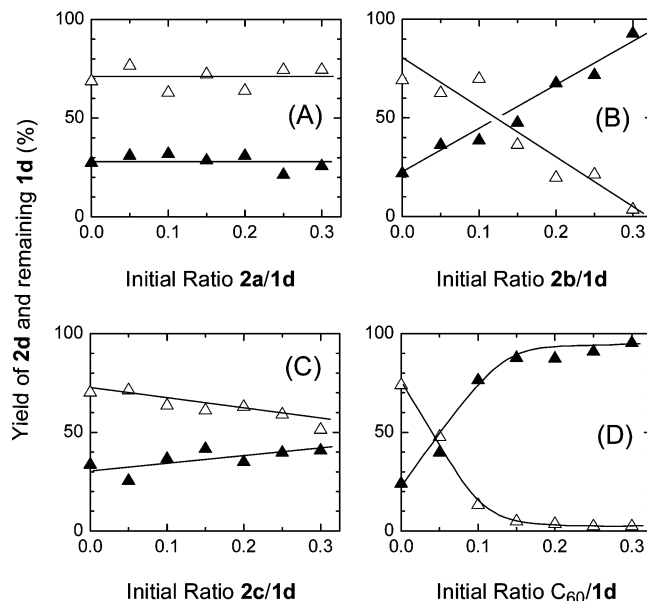


Figure 8. Yield of **2d** and remaining **1d** in degassed solutions as a function of the ratio of the amount of initially added authentic **2a** to **1d** (A), **2b** to **1d** (B), **2c** to **1d** (C), and C_{60} to **1d** (D).^{14a} Codification of substrate **1d** (△) and product **2d** (▲). Irradiation time: 50 s. Concentration: 1×10^{-5} M **1d** in toluene. Light source: 500 W Xe lamp, fitted with a water filter and a Toshiba UV-29 filter (>290 nm light).

the transient spectrum and to observe the expected triplet absorption because of the low substrate solubility. In contrast, the derivatives **1a,c** (Figure 9A-1,C-1) possess strong absorptions at 420, 650, and 1050 nm and a broad band at >1300 nm. The first two peaks are similar to those reported for the radical cations of arylamines,¹⁹ and the third peak matches the absorption of the radical anion of fullerene derivatives.^{18,20} Furthermore, the decay profile of the transient absorption disclosed oxygen quenching of the excited state.¹⁵ On the basis of these results, the transient spectra were tentatively attributed to the ion-pair states with triplet character, *ion-pair triplet* states. From the decay profiles, the lifetimes of the transient species of **1a** and **1c** were determined to be 4.5 and 7.4 μ s (cf. parts A-2 and C-2 of Figure 9); the lifetime of **1b** could not be obtained because its decay profile was too noisy.

Figure 10 shows the transient spectra of the products **2a–d** in toluene, whose general features are quite similar to the spectra of **1a–d**. Derivatives **2b** and **2d** absorb at 720 nm (normal triplet state), whose lifetimes were determined to be 12 and 5.0 μ s for **2b** and **2d** (cf. parts B-2 and D-2 of Figure 10). In contrast,

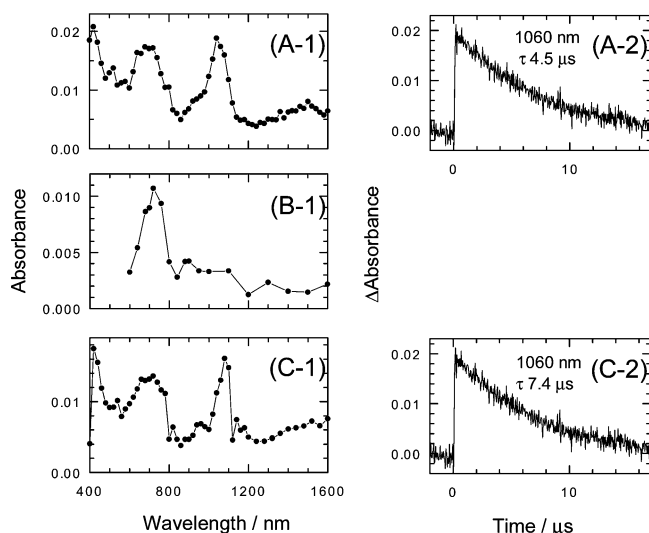


Figure 9. Nanosecond transient absorption spectra of **1a** (A-1), **1b** (B-1), and **1c** (C-1) and the decay profiles of the transient absorption peaks of **1a** (A-2) and **1c** (C-2). Excitation wavelength: 530 nm. Concentration: 10^{-4} M in toluene. Transient absorption spectra were measured at 200 ns (A, C) and 100 ns (B) after the laser pulse.

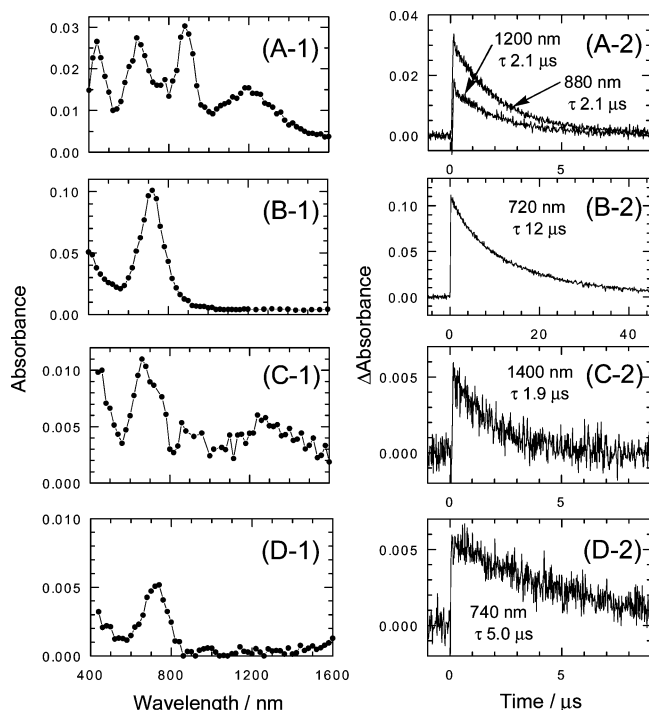


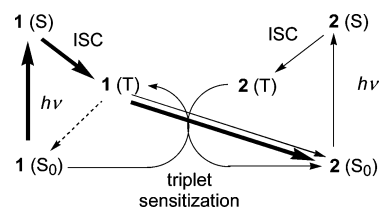
Figure 10. Nanosecond transient absorption spectra of **2a** (A-1), **2b** (B-1), **2c** (C-1), **2d** (D-1), and the corresponding decay profiles of the transient absorption peaks of **2a** (A-2), **2b** (B-2), **2c** (C-2), and **2d** (D-2). Excitation wavelength: 530 nm (A, C, D) and 532 nm (B). Concentration: 10^{-4} M in toluene. Transient absorption spectra were measured at 200 ns after the laser pulse.

products **2a** and **2c**, which have been tentatively assigned to ion-pair triplet states, possess peaks at 450, 650, and 800 nm and a broad absorption at 1250 nm. The lifetimes of **2a** and **2c** were determined to be 2.1 and 1.9 μs (cf. parts A-2 and C-2 of Figure 10), which are much shorter than the normal triplet states of **2b** and **2d**.

Discussion

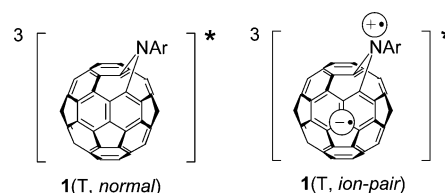
Despite the small difference in the structure of the *N*-substituted aryl groups, a large difference in the rate of

SCHEME 2



photochemical rearrangement **1** \rightarrow **2** was observed. These results are tentatively explained in terms of the various photochemical pathways in Scheme 2.

Direct Photochemical Rearrangement. Despite the large difference in the photochemical reactivities observed for the substrates **1a–d**, the computed ground-state heats of formation and the charge distribution on the nitrogen atom were similar in the PM3 level.¹⁵ Thus, the large variation in the photochemical reactivity implies considerable differences in the nature of the excited states that are involved, which are most likely due to electronic and/or structural effects of the substituents. Since the reaction proceeds through triplet states, transient absorption spectra showed that **1b**, and most likely also **1d**, possess normal triplet states. In contrast, the excited states of **1a,c** are assigned to ion-pair triplet states because the transient absorption spectra of **1a,c** are similar to those of fullerene derivatives with intramolecular charge separation^{18,20} and the excited states are quenched by oxygen.¹⁵



The fast photochemical rearrangement of **1b,d** proceeds through the triplet reaction path **1**(S_0) \rightarrow **1**(S) \rightarrow **1**(T , normal) \rightarrow **2**(S_0), shown in bold solid arrows in Scheme 2. The slow reactions of **1a,c** follow the same reaction path, but with a different triplet state, namely **1**(S_0) \rightarrow **1**(S) \rightarrow **1**(T , ion-pair) \rightarrow **2**(S_0). The photochemical experiments indicate that for **1a,c** the step **1**(T , ion-pair) \rightarrow **2**(S_0) is inefficient and the major step is **1**(T , ion-pair) \rightarrow **1**(S_0), as shown by the broken arrow in Scheme 2.

Triplet-Sensitized Photochemical Rearrangement and the Triplet Energy Levels. In contrast to the exponential reaction rates of **1a,c,d**, substrate **1b** proceeds nonexponentially (cf. Figures 3 and 4). Presumably, the nonexponential reaction involves triplet sensitization by the product **2b** since the energy of the triplet state of **2** is reported to be slightly higher than that of **1**.⁷ This triplet-sensitization mechanism of **2b** is coded with light solid arrows in Scheme 2.

The sensitization experiments allow us to derive the relative triplet energy levels of the substrates **1a–d**, the products **2a–d**, and C_{60} . For example, from Figure 5, we conclude that the relative order of the triplet energy levels is **2a** $<$ (**1a**, **1b**) $<$ (**2b**, **2c**) $<$ **1c**, and **2d** $<$ **1d** because **2b** sensitizes the photochemical rearrangement **1b** \rightarrow **2b**, but there is no sensitization by **2a**, **2c**, and **2d** in the rearrangement **1a**, **c**, **d** \rightarrow **2a**, **c**, **d**. Similarly, the relative order (**2b**, **2c**, **2d**, C_{60}) $<$ **1a** may be obtained from the sensitization experiments on **1a**; (**2a**, **2c**, **2d**) $<$ **1b** $<$ C_{60} from Figure 6 and the sensitization experiments on **1b**; (**2a**, **2b**, **2d**) $<$ **1c** $<$ C_{60} from Figure 7 and the sensitization experiments on **1c**; (**2a**, **2d**) $<$ **1d** $<$ (**2b**, **2c**, C_{60}) from Figure 8, whereas **2a** $<$ **2d** is determined from the

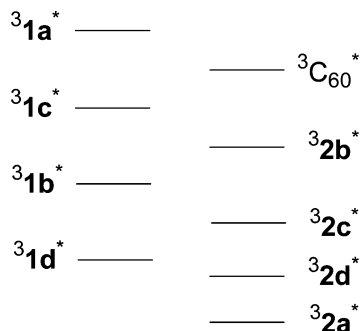


Figure 11. Relative ordering of the triplet energy levels of substrates **1a–d**, products **2a–d**, and C_{60} .

kinetic analysis of the data in Figures 3 and 4. The relative ordering of the triplet energy levels for all the compounds is summarized in Figure 11.

Although **2d** possesses a normal triplet state according to transient absorption, the lack of sensitization by **2d** may be due to the higher triplet energy level of **1d** than **2d**, as displayed in Figure 11. Alternatively, other energy dissipation paths may operate for **1d** and **2d**.

The transient spectra of **2a** and **2c** are similar to those of **1a** and **1c**; therefore, the excited states of **2a,c** are also tentatively assigned to the ion-pair triplet states. The absence of triplet sensitization in the photochemical rearrangement of **1a,c** indicates that the triplet energies of **2a** and **2c** (T, *ion-pair*) are lower than of **1a** and **2c** (T, *ion-pair*).

Although the normal triplet energy level of the rearrangement product **2** is reported to be higher than that of substrate **1**,⁷ the relative ordering in Figure 11 reveals that the triplet energy of **2** is not always higher than that of the corresponding **1**. This may be due to a considerable decrease in the triplet energy level by the ion-pair triplet.

Contribution of the Direct and Sensitized Processes. To understand the substituent effect on the photochemical rearrangement, we have conducted a kinetic analysis to assess the relative contribution of the direct and sensitized processes in the rearrangement. As photochemical conversion $\mathbf{1} \rightarrow \mathbf{2}$ proceeded quantitatively, the consumption of **1** is presented by the kinetic expression in eq 1, where $[1]_t$ and $[2]_t$ are the concentrations of **1** and **2** at time t , and k_d and k_s are the rate constants of the direct and sensitized processes. The first term of the right side of eq 1 represents the consumption of **1** by the direct photolysis and the second term for the sensitized process. Since $[2]_t = [1]_0 - [1]_t$, where $[1]_0$ is the initial concentration of **1**, the integrated form of eq 1 is given by eq 2.²¹

$$-\frac{d[1]_t}{dt} = k_d[1]_t + k_s[1]_t[2]_t \quad (1)$$

$$[1]_t = \frac{1}{\left(\frac{1}{[1]_0} - \frac{k_s}{k_d + k_s[1]_0}\right) \exp\{(k_d + k_s[1]_0)t\} + \frac{k_s}{k_d + k_s[1]_0}} \quad (2)$$

The results of the kinetic analysis by means of eq 2 are displayed in Figure 12. The symbols give the experimental consumption of **1a–d** by >290 nm light irradiation, and the lines are obtained by curve fittings²² of the data points according to eq 2; the k_d and k_s values are summarized in Table 1. Table 1 also shows the values k_d and k_s obtained similarly from the data of the >600 nm light irradiations.^{15,22}

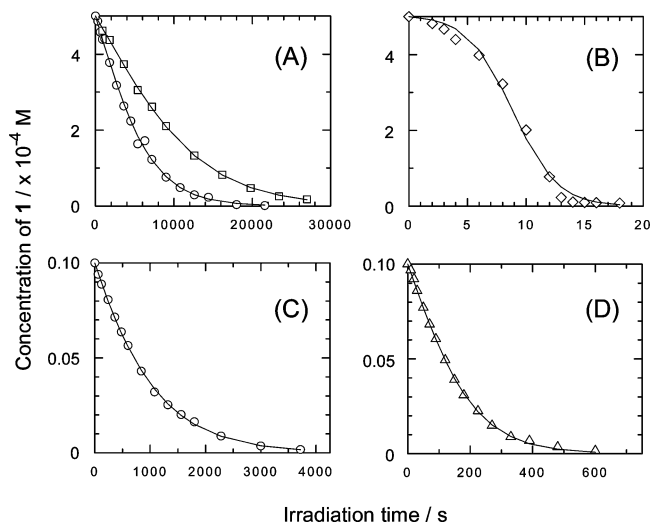


Figure 12. Decrease of **1a–d** as a function of irradiation time with curve fitting according to eq 2. Codification of substrate: **1a** (○), **1b** (◇), **1c** (□), **d** (△). Initial concentration ($[1]_0$): 5×10^{-4} (A, B) and 1×10^{-5} M (C, D) in toluene; light source: 500 W Xe lamp, fitted with a water filter and a Toshiba UV-29 filter (>290 nm light).

TABLE 1: Experimental and Curve-Fitted k_d and k_s Values of the **1a–d Derivatives According to Eq 2**

entry	wavelength (nm)	initial concn ($\times 10^{-4}$ M)	substrate	k_d^a ($\times 10^{-5}$ s $^{-1}$)	k_s^a (s $^{-1}$ M $^{-1}$)
1	>290	5.0	1a	14 (1)	0.28 (1)
2			1b	500 (36)	1040 (3714)
3			1c	7 (0.5)	0.16 (0.6)
4		0.1	1a	91 (1)	27 (1)
5			1d	471 (5.2)	443 (16)
6	>600	5.0	1a	5 (1)	0.028 (1)
7			1b	290 (58)	230 (8214)
8			1c	2 (0.4)	0.020 (0.7)
9		0.1	1a	11 (1)	12 (1)
10			1d	36 (3.3)	63 (5.3)

^a The numbers in the parentheses are the values relative to **1a**.

The rate constants k_d and k_s depend on the molar absorption coefficient (ϵ). In the cases of >290 nm light photolysis, the light is mostly absorbed by the allowed transitions of **1a–d** and **2a–d** at λ_{\max} 350 nm, whose ϵ values are similar in this wavelength region (cf. Figure 1). Therefore, when the same photolysis conditions were used, k_d and k_s reflect the initial photochemical reactivity of **1a–d**. The k_d values of entries 1–3 in Table 1 are 36- and 72-fold faster than those of **1a** and **1c** for the direct photolysis of **1b**. The k_s values indicate that the sensitized photolysis of **1b** proceeded 3700- and 6200-fold faster than those of **1a** and **1c**. The contribution of the triplet sensitization in the photochemical rearrangement $\mathbf{1} \rightarrow \mathbf{2}$ matches the triplet energy in Figure 11.

Similarly, the entries 4 and 5 indicate that the direct and sensitized reactions of **1d** proceed 5.2- and 16-fold faster than those of **1a**. Despite the fact that the nonexponential nature of the reaction (evidence for the triplet sensitization) was not definite in Figure 3, the k_s value of entry 5 (relative value is 16) indicates some triplet sensitization in the photochemical rearrangement $\mathbf{1d} \rightarrow \mathbf{2d}$; however, the contribution of the sensitization in the rearrangement $\mathbf{1d} \rightarrow \mathbf{2d}$ is only about 0.4% of that of $\mathbf{1b} \rightarrow \mathbf{2b}$.

Entries 6–10 give the k_d and k_s values in the photolysis with >600 nm light, whose relative magnitudes vary about 100- and 10 000-fold. The absorption by **1a–d** and **2a–d** in this wavelength region is due to the forbidden transitions, and as seen in Figure 1, the ϵ values differs in this wavelength region.

This fact implies that **1a–d** have different effect of ϵ on the k_d and k_s values so that the difference in the relative values cannot be explained only by the wavelength effects. However, obtained relative values were similar to those in the photolysis with >290 nm light, which indicates that the effect of ϵ on k_d and k_s values is quite small.

Our results show that the small structural differences in the *N*-substituent of fulleroids are responsible for the involvement of distinct excited states, which induce large differences in the reactivity (more than 2200-fold) of fulleroids, whose reaction center is remote from the *N*-substituent. This first-time observation in fullerene chemistry may be the consequence of the relative spatial orientation of the *N*-amino aryl and fullerene functionalities. This fact may be generalized to other molecules that have two distinct chromophores in different spatial orientations, a phenomenon that may have potential for developing novel chemistry, e.g., the application of fullerene derivatives as nanoswitches, in which the switching is accomplished through small structural variations of the molecule by varying remote substituents.

Conclusion

In conclusion, the photochemical rearrangement of 1,6-(*N*-aryl)aza-[60]fulleroids (**1**) to 1,2-(*N*-arylaziridino)-[60]fullerenes (**2**) depends on the type of *N*-aryl substituents, remote from the reaction center. A systematic study on the *N*-substituent effect by phenyl (**1a**), 1-naphthyl (**1b**), 2-naphthyl (**1c**), and 1-pyrenyl (**1d**) groups shows a large substituent effect on the rates of the photochemical rearrangement, in which the rates between the fastest (**1b**) and the slowest (**1c**) differs by ca. 2200-fold. The decreasing order of the reaction rates is 1-naphthyl (**1b**) $>$ 1-pyrenyl (**1d**) $>$ phenyl (**1a**) $>$ 2-naphthyl (**1c**). The fast photochemical rearrangement proceeds through noraml triplet states of **1** and triplet sensitization by the product **2b** in the case of **1b**. The rate constants for the direct photochemical and sensitized rearrangement were obtained by kinetic analysis of the reaction. The slow reaction of **1a,c** is interpreted by the participation of different triplet states from the normal ones, which tentatively assigned to ion-pair triplet states. The relative ordering of the triplet energy levels of **1a–d**, **2a–d**, and C_{60} , obtained by sensitization, increases in the order **2a** $<$ **2d** $<$ **1d** $<$ **2c** $<$ **1b** $<$ **2b** $<$ **1c** $<$ C_{60} $<$ **1a**. These results indicate that a small structural difference of the substrate amplifies enormously the reactivity (more than 2200-fold) through switching between the two distinct triplet excited states.

Experimental Section

Synthesis of 1,6-(*N*-Aryl)aza-[60]fulleroids (1**). General Procedure.** A sample of 500 mg of C_{60} was dissolved in 30 mL of 1,2-dichlorobenzene (DCB), and 1.5 equiv of the aryl azide in DCB was added dropwise to the stirred solution at room temperature under a nitrogen atmosphere. The reaction mixture was then stirred at 80 °C, after cooling to room temperature, 130 mL of acetonitrile was added, the precipitate was separated by centrifugation, and the solvent was passed through a PTFE membrane filter (pore size 0.45 μ m) to collect any remaining small particles. The centrifuged and filtered precipitates were combined and then submitted to silica gel chromatography (1:1 mixture of CS_2 :*n*-hexane as eluent) to give pure **1** and recovered C_{60} . Experimental details, analytical data, and spectral data of **1a–d** are given in the Supporting Information.

Synthesis of 1,2-(*N*-Arylaziridino)-[60]fullerenes (2**). General Procedure.** A sample of **1** was dissolved in toluene, and nitrogen gas was passed through the stirred solution for an

appropriate time. The stirred solution was then irradiated with a 500 W xenon lamp (USHIO Optical ModuleX SX-UI500XQ), supplied with an 18 cm water filter and a Toshiba UV-29 filter under a nitrogen gas atmosphere in a Pyrex vessel. The reaction mixture was then submitted to silica gel chromatography (1:1 mixture of CS_2 :*n*-hexane as eluent) to give pure **2**. The experimental details, analytical data, and the spectral data of **2a–d** are given in the Supporting Information.

Photolysis of 1,6-(*N*-Aryl)aza-[60]fulleroids (1a–d**).** The toluene (spectral grade) solutions of **1** [5×10^{-4} M (**1a–c**) and 1×10^{-5} M (**1a, d**)] were prepared and degassed by three freeze–pump–thaw cycles. The photolysis of **1** was conducted in a 20 mL Pyrex round-bottomed flask under a nitrogen-gas atmosphere while stirring. A 500 W xenon lamp, fitted with an 18 cm water filter (output energy after the water filter was 9.6–9.8 mW cm^{-2}) and a Toshiba UV-29, Y-45, or R-60 filter, was used for the photolysis. The photolyses of **1** in air-saturated and nitrogen-purged solutions were conducted under the same experimental conditions; the solution were stirred under the air or nitrogen gas for 2 h. The consumption of **1** and the formation of **2** were determined by HPLC analysis [RP-18e column (4 mm i.d. \times 250 mm); UV/vis detector wavelength: 300 nm], relative to authentic samples.

Photolysis of 1,6-(*N*-Aryl)aza-[60]fulleroids (1a–d**) in the Presence of 1,2-(*N*-Arylaziridino)-[60]fullerenes (**2a–d**) or C_{60} .** The toluene (spectral grade) solutions of **1** [5×10^{-4} M (**1a–c**) and 1×10^{-5} M (**1d**)] and **2** [$0–1.5 \times 10^{-4}$ M (**2a–c**) and $0–3 \times 10^{-6}$ M (**2d**)] were prepared and degassed by three freeze–pump–thaw cycles. The photolysis was conducted by using the same experimental conditions as these for the photolysis of **1**. The consumption of **1** and the formation of **2** were determined by the same analytical system as that used for the photolysis of **1**. The results are the average of three or four independent runs.

Flash Photolysis of **1 and **2**.** Transient absorption spectra in the visible/near-IR regions were observed by the laser-flash photolysis spectroscopy. The C_{60} derivatives were excited with 530–532 nm light from the OPO system, attached to a Nd:YAG laser (6 ns fwhm). A Si–PIN photodiode module (400–600 nm) and a Ge-APD module (600–1600 nm) were employed as detectors for monitoring the light from a pulsed Xe lamp.^{18f}

Acknowledgment. We thank Mr. S. Kawabata, Mr. M. Yamaguchi, and Mr. A. Tominaga, Shimadzu Co., for MALDI–TOFMS measurements, Dr. H. Sakai for 500 MHz NMR measurements, and Dr. P. K. Drechsel for the preparation of **1a**. We thank Professor W. Adam for going through the manuscript. Y.A. and O.I. are grateful for financial support by a Grant-in-Aid of Scientific Research on Priority Areas (417) from the Ministry of Education, Culture, Sports, Science, and Technology of Japan.

Supporting Information Available: Preparation of phenyl azide, 1- and 2-naphthyl azides, and 1-pyrenyl azide; experimental details, analytical data, and spectral data of **1a–d** and **2a–d**; derivation of eq 2 from eq 1; results on the photochemical rearrangement of **1a–d** under air-saturated conditions, photolysis of **1a–c** under nitrogen-purged conditions, and photolysis of **1a–d** with >450 nm light under degassed conditions; the effects of **2b** addition in the photochemical rearrangement **1b** \rightarrow **2b** with >600 nm light, of **2b–d** and C_{60} addition in the rearrangement **1a** \rightarrow **2a** with >290 nm light, of **2a,c,d** and C_{60} addition in the rearrangement **1b** \rightarrow **2b** with >290 nm light, and of **2a,b,d** and C_{60} addition in the rearrangement **1c** \rightarrow **2c**

with >290 nm light; the decay profiles of the transient absorption peaks of **1a** and **2a** in the absence and presence of oxygen gas; curve fitting of the data on the consumption of **1a–d** by >600 nm light irradiation according to eq 2; PM3 calculation on the ground-state heats of formation and the charges on the nitrogen atom for **1** and **2**. This material is available free of charge via the Internet at <http://pubs.acs.org>.

References and Notes

(1) (a) Hirsch, A. *The Chemistry of the Fullerenes*; Georg Thieme Verlag: Stuttgart, 1994. (b) Taylor, R. *Lecture Notes on Fullerene Chemistry: A Handbook for Chemists*; Imperial College Press: London, 1999.

(2) (a) Foote, C. S. *Top. Curr. Chem.* **1994**, *169*, 347–363. (b) Sun, Y.-P. *Mol. Supramol. Photochem.* **1997**, *1*, 325–390. (c) Mattay, J.; Siedschlag, C.; Torres-Garcia, G.; Ulmer, L.; Wolff, C.; Fujitsuka, M.; Watanabe, A.; Ito, O.; Luftmann, H. *Proc. Electrochem. Soc.* **1997**, *97–14*, 326–337. (d) Mattay, J.; Ulmer, L.; Sotzmann, A. *Mol. Supramol. Photochem.* **2001**, *8*, 637–752. (e) Fukuzumi, S.; Guldi, D. M. *Electron Transfer in Chemistry*; Balzani, V., Ed.; Wiley-VCH: Weinheim, 2001; Vol. II, Part I, p 270. (f) Kleineweischede, A.; Mattay, J. Photochemical Reaction of Fullerenes and Fullerene Derivatives. In *CRC Handbook of Organic Photochemistry Photobiology*, 2nd ed.; Horspool, W., Lenci, F., Eds.; CRC Press: Boca Raton, FL, 2003; Chapter 28.

(3) (a) Prato, M.; Li, Q. C.; Wudl, F.; Lucchini, V. *J. Am. Chem. Soc.* **1993**, *115*, 1148–1150. (b) Yan, M.; Cai, S. X.; Keana, J. F. W. *J. Org. Chem.* **1994**, *59*, 5951–5954. (c) Hummelen, J. C.; Prato, M.; Wudl, F. *J. Am. Chem. Soc.* **1995**, *117*, 7003–7004. (d) Grösser, T.; Prato, M.; Lucchini, V.; Hirsch, A.; Wudl, F. *Angew. Chem., Int. Ed. Engl.* **1995**, *34*, 1343–1345. (e) Lamparth, I.; Nuber, B.; Schick, G.; Skiebe, A.; Grösser, T.; Hirsch, A. *Angew. Chem., Int. Ed. Engl.* **1995**, *34*, 2257–2259. (f) Hummelen, J. C.; Knight, B.; Pavlovich, J.; González, R.; Wudl, F. *Science* **1995**, *269*, 1554–1556. (g) Averdug, J.; Mattay, J. *Tetrahedron* **1996**, *52*, 5407–5420. (h) Jagerovic, N.; Elguero, J.; Aubagnac, J.-L. *Tetrahedron* **1996**, *52*, 6733–6738. (i) Bellavia-Lund, C.; Wudl, F. *J. Am. Chem. Soc.* **1997**, *119*, 943–946. (j) Shen, C. K.-F.; Yu, H.; Juo, C.-G.; Chien, K.-M.; Her, G.-R.; Luh, T.-Y. *Chem.—Eur. J.* **1997**, *3*, 744–748. (k) Kanakamma, P. P.; Huang, S.-L.; Juo, C.-G.; Her, G.-R.; Luh, T.-Y. *Chem.—Eur. J.* **1998**, *4*, 2037–2042. (l) Schick, G.; Jarrosson, T.; Rubin, Y. *Angew. Chem., Int. Ed. Engl.* **1999**, *38*, 2360–2363. (m) Iglesias, M.; Gómez-Lor, B.; Santos, A. *J. Organomet. Chem.* **2000**, *599*, 8–17. (n) Cases, M.; Duran, M.; Mestres, J.; Martín, N.; Solà, M. *J. Org. Chem.* **2001**, *66*, 433–442. (o) Ulmer, L.; Mattay, J. *Eur. J. Org. Chem.* **2003**, 2933–2940.

(4) (a) Banks, M. R.; Cadogan, J. I. G.; Gosney, I.; Hodgson, P. K. G.; Langridge-Smith, P. R. R.; Millar, J. R. A.; Taylor, A. T. *Tetrahedron Lett.* **1994**, *35*, 9067–9070. (b) Ishida, T.; Tanaka, K.; Nogami, T. *Chem. Lett.* **1994**, 561–562. (c) Averdug, J.; Mattay, J.; Jacobi, D.; Abraham, W. *Tetrahedron* **1995**, *51*, 2543–2552. (d) Banks, M. R.; Cadogan, J. I. G.; Gosney, I.; Hodgson, P. K. G.; Langridge-Smith, P. R. R.; Millar, J. R. A.; Parkinson, J. A.; Rankin, D. W. H.; Taylor, A. T. *J. Chem. Soc., Chem. Commun.* **1995**, 887–888. (e) Schick, G.; Grösser, T.; Hirsch, A. *J. Chem. Soc., Chem. Commun.* **1995**, 2289–2290. (f) Shiu, L.-L.; Chien, K.-M.; Liu, T.-Y.; Lin, T.-I.; Her, G.-R.; Luh, T.-Y. *J. Chem. Soc., Chem. Commun.* **1995**, 1159–1160. (g) Dong, G.-X.; Li, J.-S.; Chan, T.-H. *J. Chem. Soc., Chem. Commun.* **1995**, 1725–1726. (h) Averdug, J.; Luftmann, H.; Schlachter, I.; Mattay, J. *Tetrahedron* **1995**, *51*, 6977–6982. (i) Smith, III, A. B.; Tokuyama, H. *Tetrahedron* **1996**, *52*, 5257–5262. (j) Schick, G.; Hirsch, A.; Mauser, H.; Clark, T. *Chem.—Eur. J.* **1996**, *2*, 935–943. (k) Banks, M. R.; Cadogan, J. I. G.; Gosney, I.; Henderson, A. J.; Hodgson, P. K. G.; Kerr, W. G.; Kerth, A.; Langridge-Smith, P. R. R.; Millar, J. R. A.; Mount, A. R.; Parkinson, J. A.; Taylor, A. T.; Thornburn, P. *Chem. Commun.* **1996**, 507–508. (l) Averdug, J.; Wolff, C.; Mattay, J. *Tetrahedron Lett.* **1996**, *37*, 4683–4684. (m) Rubin, Y. *Chem.—Eur. J.* **1997**, *3*, 1009–1016.

(5) (a) Hawker, C. J.; Wooley, K. L.; Fréchet, J. M. J. *J. Chem. Soc., Chem. Commun.* **1994**, 925–926. (b) Takeshita, M.; Suzuki, T.; Shinkai, S. *J. Chem. Soc., Chem. Commun.* **1994**, 2587–2588. (c) Hawker, C. J.; Saville, P. M.; White, J. W. *J. Org. Chem.* **1994**, *59*, 3503–3505. (d) Wang, N.; Li, J.; Zhu, D. *Tetrahedron Lett.* **1995**, *36*, 431–434. (e) Shen, C. K.-F.; Chien, K.-M.; Juo, C.-G.; Her, G.-R.; Luh, T.-Y. *J. Org. Chem.* **1996**, *61*, 9242–9244. (f) Zhou, J.; Rieker, A.; Grösser, T.; Skiebe, A.; Hirsch, A. *J. Chem. Soc., Perkin Trans. 2* **1997**, 1–5. (g) Yashiro, A.; Nishida, Y.; Ohno, M.; Eguchi, S.; Kobayashi, K. *Tetrahedron Lett.* **1998**, *39*, 9031–9034. (h) Yashiro, A.; Nishida, Y.; Ohno, M.; Eguchi, S.; Kobayashi, K. *Tetrahedron Lett.* **1998**, *39*, 9031–9034. (i) Shon, T.-S.; Kelly, K. F.; Halas, N. J.; Lee, T. R. *Langmuir* **1999**, *15*, 5329–5332. (j) Prato, M. *Top. Curr. Chem.* **1999**, *199*, 173–187. (k) Ikeda, A.; Fukuhara, C.; Kawaguchi, M.; Numata, M.; Shinkai, S.; Liu, S.-G.; Echegoyen, L. *J. Chem. Soc., Perkin Trans. 2* **2000**, 307–310. (l) Iglesias, M.; Gómez-Lor, B.; Santos, A. *J. Organomet. Chem.* **2001**, *627*, 159–166. (m) Du, C.; Xu, B.; Li, Y.; Wang,

C.; Wang, S.; Shi, Z.; Fang, H.; Xiao, S.; Zhu, D. *New J. Chem.* **2001**, *25*, 1191–1194. (n) Yuan, D.-Q.; Koga, K.; Kourogi, Y.; Fujita, K. *Tetrahedron Lett.* **2001**, *42*, 6727–6729. (o) Xiao, S.; Li, Y.; Fang, H.; Li, H.; Liu, H.; Shi, Z.; Jiang, L.; Zhu, D. *Org. Lett.* **2002**, *4*, 3063–3066. (p) González, S.; Martín, N.; Swartz, A.; Guldi, D. M. *Org. Lett.* **2003**, *5*, 557–560.

(6) (a) Hasharoni, K.; Keshavarz-K. M.; Sastre, A.; González, R.; Bellavia-Lund, C.; Greenwald, Y.; Swager, T.; Wudl, F.; Heeger, A. J. *J. Chem. Phys.* **1997**, *107*, 2308–2312. (b) Delpoux, S.; Beguin, F.; Benoit, R.; Erre, R.; Manolova, N.; Rashkov, I. *Eur. Polym. J.* **1998**, *34*, 905–915. (c) Taton, D.; Angot, S.; Gnanou, Y.; Wolert, E.; Setz, S.; Duran, R. *Macromolecules* **1998**, *31*, 6030–6033. (d) Yuanyin, C.; Pengfei, F.; Zhao, Z.; Jianhong, F. *Chem. Lett.* **1999**, 499–500. (e) Cloutet, E.; Fillaut, J.-L.; Astruc, D.; Gnanou, Y. *Macromolecules* **1999**, *32*, 1043–1054. (f) Huang, X. D.; Goh, S. H. *Macromolecules* **2000**, *33*, 8894–8897. (g) Zheng, J. Z.; Goh, S. H.; Lee, S. Y. *J. Appl. Polym. Sci.* **2000**, *75*, 1393–1396. (h) Huang, X. D.; Goh, S. H. *Macromolecules* **2001**, *34*, 3302–3307. (i) Wang, S.; Xiao, S.; Li, Y.; Shi, Z.; Du, C.; Fang, H.; Zhu, D. *Polymer* **2002**, *43*, 2049–2054. (j) Wang, S.; Yang, J.; Li, Y.; Lin, H.; Guo, Z.; Xiao, S.; Shi, Z.; Zhu, D.; Woo, H.-S.; Carroll, D. L.; Kee, I.-S.; Lee, J.-H. *Appl. Phys. Lett.* **2002**, *80*, 3847–3849.

(7) (a) Guldi, D. M.; Carmichael, I.; Hungerbühler, H.; Asmus, K.-D.; Maggini, M. *Proc. Electrochem. Soc.* **1998**, *98–8*, 268–272. (b) Guldi, D. M.; Hungerbühler, H.; Carmichael, I.; Asmus, K.-D.; Maggini, M. *J. Phys. Chem. A* **2000**, *104*, 8601–8608.

(8) (a) Diederich, F.; Isaacs, L.; Philip, D. *Chem. Soc. Rev.* **1994**, 243–255. (b) Diederich, F.; Thilgen, C. *Science* **1996**, *271*, 317–323. (c) Hall, M. H.; Lu, H.; Shevlin, P. B. *J. Am. Chem. Soc.* **2001**, *123*, 1349–1354.

(9) Preliminary results: Ouchi, A.; Hatsuda, R.; Awen, B. Z. S.; Sakuragi, M.; Ogura, R.; Ishii, T.; Araki, Y.; Ito, O. *J. Am. Chem. Soc.* **2002**, *124*, 13364–13365.

(10) (a) The yields of **1** and recovered C₆₀ are based on the amount of initially used C₆₀. (b) The yields of **2** are based on the amount of initially used **1**. The yields of **2** have not been optimized.

(11) Leach, S.; Vervloet, M.; Desprès, A.; Bréheret, E.; Hare, J. P.; Dennis, T. J.; Kroto, H. W.; Taylor, R.; Walton, D. R. M. *Chem. Phys.* **1992**, *160*, 451–466.

(12) Rath, M. C.; Pal, H.; Mukherjee, T. *J. Phys. Chem. A* **1999**, *103*, 4993–5002.

(13) E.g.: Luo, C.; Fujitsuka, M.; Watanabe, A.; Ito, O.; Gau, L.; Huang, Y.; Huang, C.-H. *J. Chem. Soc., Faraday Trans.* **1998**, *94*, 527–532.

(14) The results were obtained (a) from one independent run or (b) from the average of two or (c) three or (d) four independent runs.

(15) The experimental results are given in the Supporting Information.

(16) Arbogast, J. W.; Darmanyan, A. P.; Foote, C. S.; Rubin, Y.; Diederich, F. N.; Alvarez, M. M.; Anz, S. J.; Whetten, R. L. *J. Phys. Chem.* **1991**, *95*, 11–12.

(17) E.g.: (a) Sension, R. J.; Szarka, A. Z.; Smith, G. R.; Hochstrasser, R. M. *Chem. Phys. Lett.* **1991**, *185*, 179–183. (b) Sension, R. J.; Phillips, C. M.; Szarka, A. Z.; Romanow, W. J.; Macghe, A. R.; McCauley, J. P.; Smith, III, Jr., A. B.; Hochstrasser, R. M. *J. Phys. Chem.* **1991**, *95*, 6075–6081. (c) Greaney, M. A.; Gorun, S. M. *J. Phys. Chem.* **1991**, *95*, 7142–7144. (d) Dimitrijevic, N. M.; Kamat, P. V. *J. Phys. Chem.* **1992**, *96*, 4811–4814. (e) Gasyna, Z.; Andrews, L.; Schatz, P. N. *J. Phys. Chem.* **1992**, *96*, 1525–1527. (f) Ghosh, H. N.; Pal, H.; Sapre, A. V.; Mittal, J. P. *J. Am. Chem. Soc.* **1993**, *115*, 11722–11727. (g) Guldi, D. M.; González, S.; Martín, N.; Antón, A.; Garín, J.; Orduna, J. *J. Org. Chem.* **2000**, *65*, 1978–1983.

(18) (a) Thomas, K. G.; Biju, V.; Guldi, D. M.; Kamat, P. V.; George, M. V. *J. Phys. Chem. B* **1999**, *103*, 8864–8869. (b) Konishi, T.; Fujitsuka, M.; Ito, O.; Toba, Y.; Usui, Y. *J. Phys. Chem. A* **1999**, *103*, 9938–9942. (c) Konishi, T.; Sasaki, Y.; Fujitsuka, M.; Toba, Y.; Moriyama, H.; Ito, O. *J. Chem. Soc., Perkin Trans. 2* **1999**, 551–556. (d) Martín, N.; Sánchez, L.; Herranz, M. A.; Guldi, D. M. *J. Phys. Chem. A* **2000**, *104*, 4648–4657. (e) Bhasikuttan, A. C.; Shastri, L. V.; Sapre, A. V. *J. Photochem. Photobiol. A: Chem.* **2001**, *143*, 17–21. (f) Yamazaki, M.; Araki, Y.; Fujitsuka, M.; Ito, O. *J. Phys. Chem. A* **2001**, *105*, 8615–8622. (g) Imahori, H.; El-Khouly, M. E.; Fujitsuka, M.; Ito, O.; Sakata, Y.; Fukuzumi, S. *J. Phys. Chem. A* **2001**, *105*, 325–332. (h) El-Khouly, M. E.; Araki, Y.; Fujitsuka, M.; Ito, O. *Phys. Chem. Chem. Phys.* **2002**, *4*, 3322–3329. (i) Ito, O.; Sasaki, Y.; El-Khouly, M. E.; Araki, Y.; Fujitsuka, M.; Hirao, A.; Nishizawa, H. *Bull. Chem. Soc. Jpn.* **2002**, *75*, 1247–1254. (j) Nakanishi, I.; Fukuzumi, S.; Konishi, T.; Ohkubo, K.; Fujitsuka, M.; Ito, O.; Miyata, N. *J. Phys. Chem. B* **2002**, *106*, 2372–2380. (k) Nakanishi, I.; Ohkubo, K.; Fujita, S.; Fukuzumi, S.; Konishi, T.; Fujitsuka, M.; Ito, O.; Miyata, N. *J. Chem. Soc., Perkin Trans. 2* **2002**, 1829–1833. (l) Murakami, H.; Matsumoto, R.; Okusa, Y.; Sagara, T.; Fujitsuka, M.; Ito, O.; Nakashima, N. *J. Mater. Chem.* **2002**, *12*, 2026–2033. (m) Fujitsuka, M.; Makinoshima, T.; Ito, O.; Obara, Y.; Aso, Y.; Otsubo, T. *J. Phys. Chem. B* **2003**, *107*, 739–746.

(19) Shida, T. *Electronic Absorption Spectra of Radical Ions*; Elsevier: Amsterdam, 1988.

(20) (a) Guldi, D. M.; Maggini, M.; Scorrano, G.; Prato, M. *J. Am. Chem. Soc.* **1997**, *119*, 974–980. (b) Fujitsuka, M.; Toba, Y.; Yamashiro, T.; Aso,

Y.; Otsubo, T. *J. Phys. Chem. A* **2000**, *104*, 4876–4881. (c) Fukuzumi, S.; Ohkubo, K.; Imahori, H.; Shao, J.; Ou, Z.; Zheng, G.; Chen, Y.; Pandey, R. K.; Fujitsuka, M.; Ito, O.; Kadish, K. M. *J. Am. Chem. Soc.* **2001**, *123*, 10676–10683. (d) Imahori, H.; Tamaki, K.; Araki, Y.; Sekiguchi, Y.; Ito, O.; Sakata, Y.; Fukuzumi, S. *J. Am. Chem. Soc.* **2002**, *124*, 5165–5174 and references therein.

(21) Derivation of eq 2 from eq 1 is given in the Supporting Information.
(22) Curve fitting was conducted by using the Levenberg–Marquardt algorithm with the ORIGIN version 6.1J computer program, produced by MICROCAL Software, Inc.
(23) The corresponding aryl azides were synthesized according to the reported procedures.¹⁵